

# MULTI-RESONATOR APPROACH TO ELIMINATING THE TEMPERATURE DEPENDENCE OF SILICON-BASED TIMING REFERENCES

Vikram A. Thakar\*, Zhengzheng Wu, Cesar Figueroa, and Mina Rais-Zadeh  
University of Michigan, Ann Arbor, USA

## ABSTRACT

This work reports on a multi-resonator system capable of generating a temperature-stable frequency reference across a wide temperature range. The system involves the use of a minimum of three temperature-compensated oscillators having a slightly different turnover temperature. The oscillator output frequency undergoes frequency multiplication and mixing in two stages to achieve a temperature-stable frequency output. The sensitivity of the clock frequency is analyzed as a function of temperature induced measurement errors.

AlN-on-silicon ring resonators actuated piezoelectrically are proposed as the three frequency setting components. Their turnover temperature is controlled through the placement of oxide within the resonator volume. A total frequency shift of less than 10 ppm is estimated across the temperature range of -40 °C to 85 °C with this implementation.

## INTRODUCTION

Timekeeping plays an important role in inertial navigation and modern communication systems. A temperature-stable frequency reference is an essential ingredient of such timing devices. Quartz-based oscillators have successfully fulfilled this need over the past few decades. As miniaturization leads to significant cost reduction, there has been a strong push to replace bulky quartz with micromachined silicon-based alternatives.

For all its merits as a mechanically robust material, moderately doped silicon suffers from a relatively large temperature-induced shift in its elastic modulus, which leads to an unacceptably large frequency fluctuation. To overcome this challenge, a number of approaches have been proposed and experimentally demonstrated [1], [2]. Passive compensation of silicon resonators has been achieved using silicon dioxide to negate the temperature dependence of silicon [3]. Due to the nature of the temperature coefficients, passive compensated silicon resonators demonstrate a parabolic temperature dependence of frequency, with the overall frequency shift limited to ~100 ppm across the industrial temperature range [4]. For more stable frequency references, the residual temperature sensitivity of silicon resonators can be actively compensated in a feedback loop with input from an on-chip temperature sensor [2].

Recently, we utilized the second-order temperature dependence

of passively compensated silicon resonators to achieve a temperature-stable frequency output [5]. This approach makes use of three temperature-compensated resonators having distinct temperature compensation profiles in a multi-resonator system, as shown in Fig.1, to generate a temperature-stable frequency reference.

Using a simple analysis we showed that for three resonators with unique second-order temperature dependence we can achieve a temperature-insensitive clock signal [5]. In this work, we extend the analysis to look at the system sensitivity to measurement errors and resonator drift. We show that resonator drift has no impact on the temperature sensitivity of the clock output, but causes a constant shift in the output frequency over time. On the other hand, calibration-induced errors are shown to cause significant temperature sensitivity in the clock output. As a consequence, sufficient care must be taken during the initial one-time calibration to ensure a temperature-insensitive clock output.

## CLOCK DESCRIPTION

Figure 1 shows a block diagram of the proposed temperature-insensitive clock. As seen from the schematic, the system utilizes three oscillators with different turnover temperatures, which is defined as the inflection point of the parabolic dependence of resonator frequency with temperature. The frequency of each oscillator can be written as

$$f_n = a_n T^2 + b_n T + c_n \quad (1)$$

Because of having different turnover temperatures, the three resonators have unique and non-zero coefficients  $a$ ,  $b$  and  $c$ . These coefficients are calculated by measuring the resonator response as a function of temperature during a one-time calibration run. The output of the three oscillators undergoes frequency multiplication and mixing in two stages to achieve a final temperature-stable frequency reference. Stage I multiplication factors  $k_1$  and  $k_3$  are set so as to ensure a purely second-order frequency dependence on temperature. At the output of the first set of mixers we can write,

$$\begin{cases} f_{12} = (k_1 a_1 + a_2) T^2 + (k_1 b_1 + b_2) T + (k_1 c_1 + c_2) \\ f_{23} = (k_3 a_3 + a_2) T^2 + (k_3 b_3 + b_2) T + (k_3 c_3 + c_2) \end{cases} \quad (2)$$

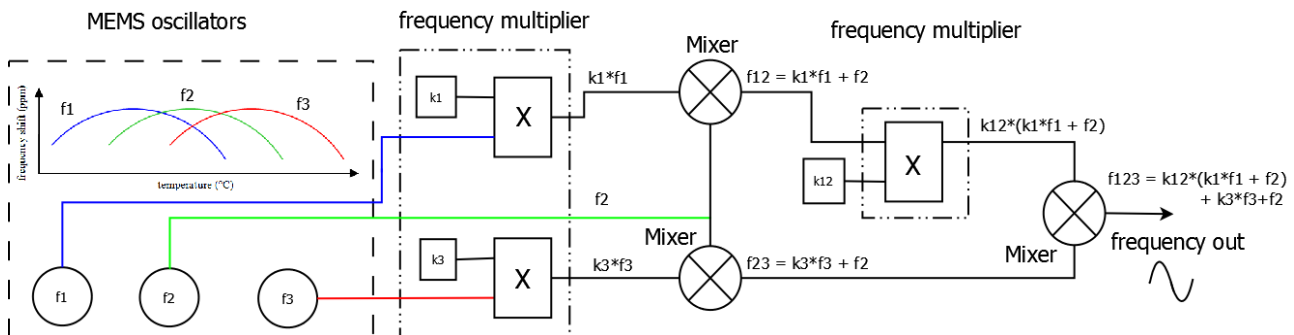


Figure 1: Algorithm for the multi-resonator temperature-stable clock. A minimum of three MEMS oscillators having different turnover temperatures are required in this implementation. The frequency multiplication is achieved using an  $n$ -fractional phase locked loop (PLL) while the frequency mixing is achieved using a mixer and a suitable filter.

The above equation sets the multipliers  $k_1$  and  $k_3$ ; to remove the first-order dependence of frequency on temperature, we have

$$k_1 = -\frac{b_2}{b_1} \text{ and } k_3 = -\frac{b_2}{b_3}. \quad (3)$$

Thus, at the input of the second mixer, the two frequency signals have a pure second-order temperature dependence, which can be compensated using a similar approach. The multiplier  $k_{12}$  is determined such that the second-order term is canceled. The parameter  $k_{12}$  can then be estimated as

$$k_{12} = -\left[\frac{k_3 a_3 + a_2}{k_1 a_1 + a_2}\right] \quad (4)$$

and the output frequency can be written as

$$f_{123} = k_{12}k_1c_1 + (1 + k_{12})c_2 + k_3c_3. \quad (5)$$

The equation for the output frequency is a combination of constants independent of temperature, and thus this system allows for the realization of a temperature-insensitive clock [5].

### SENSITIVITY TO RESONATOR DRIFT

The effect of temperature-independent frequency drift can be captured in (1) by noting,

$$f_n = a_n T^2 + b_n T + (c_n + d_n), \quad (6)$$

where  $d_n$  is temperature-independent frequency drift for the  $n^{\text{th}}$  resonator. Following the steps in the previous section the effect of individual resonator drift at the clock output can be written as,

$$(f_{123})_d = f_{123} + k_{12}k_1d_1 + (1 + k_{12})d_2 + k_3d_3. \quad (7)$$

As can be noted from (7), since  $k_1$ ,  $k_3$  and  $k_{12}$  are invariant with temperature, the resultant frequency  $(f_{123})_d$  is also independent of temperature but has a constant offset from the original calibrated output frequency.

### SENSITIVITY TO MEASUREMENT ERRORS

#### Case 1: Non-uniform temperature distribution in measurement chamber

Considering that most low-frequency resonator measurements are performed in low-vacuum conditions, it is quite possible that the measurement chamber has some temperature non-uniformity. Since the temperature controller maintains the sensor at the set temperature rather than the actual resonator temperature, this implies the resonator may either lead or lag the sensor temperature depending on the nature of the non-uniformity. This can cause an error in the measurement during the calibration process, due to which we have

$$f'_n = a'_n T^2 + b'_n T + c'_n, \quad (8)$$

whereas the real temperature dependence is given using (1). For the purpose of this analysis we can split the measured individual coefficients  $a'_n$ ,  $b'_n$  and  $c'_n$  into a real component and an error component. Then, we can express  $f'_n$  as,

$$f'_n = (a_{0n} + a_n)T^2 + (b_{0n} + b_n)T + (c_{0n} + c_n),$$

and

$$f'_n = f_n + f_{0n}. \quad (9)$$

Here,  $a_{0n}$ ,  $b_{0n}$  and  $c_{0n}$  are the respective error components for the  $n^{\text{th}}$  resonator while  $f_{0n}$  is the total frequency error for the  $n^{\text{th}}$  resonator. Again, following the same steps from (1) to (5), we can express the effect of measurement error on the system output as,

$$f'_{123} = f_{123} + k_1k_{12}f_{01} + (1 + k_{12})f_{02} + k_3f_{03} \quad (10)$$

We should note here that  $f_{0n}$  values are temperature dependent and thus the clock output too has second-order temperature dependence.

#### Case 2: Temperature sensor calibration error

In this case, while we assume the resonator to be at temperature  $T$ , in reality it is operating at temperature  $T'$ . This would lead to a simplified case of (10) wherein the turnover temperature is incorrectly estimated by  $(T-T')$  but the shape of the frequency-temperature dependence (parabola) remains unchanged. In this case, we have no change in  $a_{0n}$  and we can write

$$f_{0n} = b_{0n}T + c_{0n}. \quad (11)$$

Equations (10) and (11) given above suggest that non-idealities during measurement of the individual resonators can significantly impact the temperature sensitivity of the clock output. This is graphically represented in Fig. 2. In Fig. 2(a) the expected nature of the temperature dependence of clock frequency with temperature errors is plotted. Fig. 2(b) plots the clock output in presence of a constant temperature sensor calibration error. Results suggest that proper care must be taken during the calibration run to ensure that these errors are minimized. Once properly calibrated a temperature-insensitive clock output can be obtained.

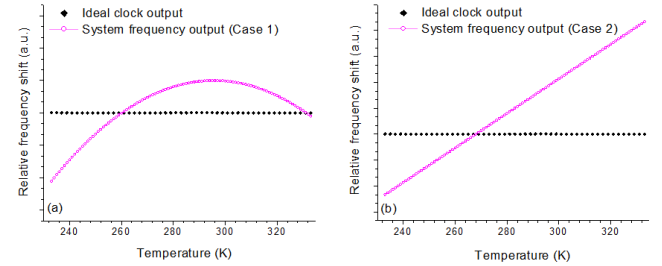


Figure 2: Graphical representation of the temperature dependence of the clock frequency output due to (a) temperature errors during measurement and (b) constant temperature sensor calibration error.

### TEMPERATURE-COMPENSATED RESONATORS

For practical demonstration of the system, it is necessary to have a minimum of three resonators demonstrating unique temperature dependence of frequency. Here we choose to use a coupled-ring or 'dogbone' resonator for their suitable characteristics [6]. Figure 3 shows a schematic of the resonator and highlights the location of the silicon dioxide islands used to achieve the temperature compensation. By moving this oxide across the width of the ring we can achieve a fine control over the resonator turnover temperature [7].

Figure 4 plots the simulated turnover temperature as a function of 'edge' spacing and shows that the turnover temperature is a strong function of the location of oxide. Using this approach we can tune the turnover temperature from  $-20$  °C to  $+80$  °C through lithography variations across the same die. No process modifications are necessary to achieve these different temperature profiles. The fabrication process flow is shown in Fig. 5.

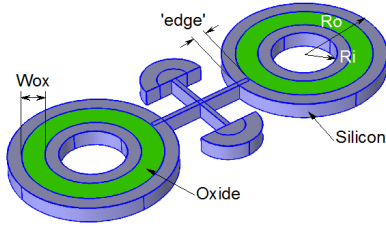


Figure 3: Schematic of a temperature-compensated coupled-ring or 'dogbone' resonator. By changing the spacing between the oxide island and the resonator boundary, we can control the turnover temperature.

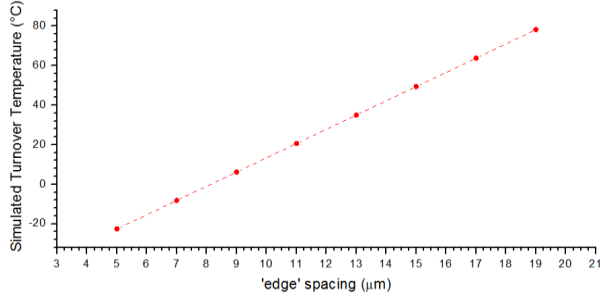


Figure 4: Simulated turnover temperature as a function of 'edge' spacing. By moving the oxide islands towards the center of the rings, the turnover temperature can be changed from  $-20^{\circ}\text{C}$  to  $+80^{\circ}\text{C}$ .

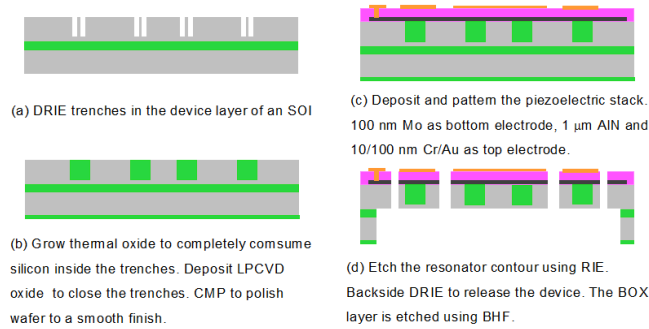


Figure 5: Process flow used to fabricate the 'dogbone' resonators [5].

Figure 6 shows two SEM images of a fabricated 'dogbone' resonator. The refilled oxide along with the 'edge' spacing can be clearly identified in Fig. 6(b). Figure 7 shows the measured frequency response of an uncompensated and a temperature-compensated ring resonator. A small degradation in the measured quality factor ( $Q$ ) is noted due to the presence of the oxide islands.

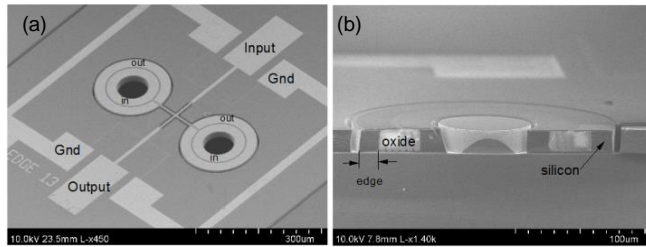


Figure 6: (a) Top SEM view of a fabricated coupled ring resonator. (b) Cross-section view showing the oxide islands within the silicon body.

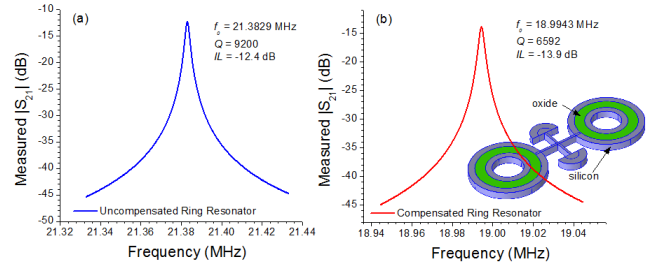


Figure 7: Measured frequency response of (a) an uncompensated and (b) a temperature-compensated ring resonator. The compensated ring resonator has an 'edge' spacing of  $17\ \mu\text{m}$ .

The temperature dependence of four temperature-compensated resonators is measured in a cryogenic probe station and is plotted in Fig. 8. Figure 8 includes two sets of measurements carried on the same devices. These results are utilized later to analyze the effect of measurement induced error on the clock output.

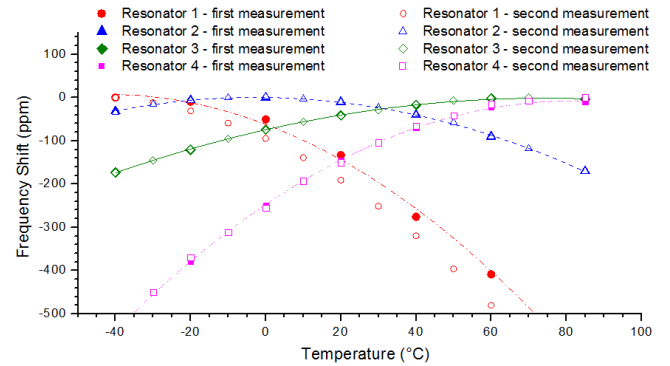


Figure 8: Measured frequency shift for four temperature-compensated ring resonators. All four resonators have the same volume of oxide but oxide trenches are placed  $7\ \mu\text{m}$ ,  $13\ \mu\text{m}$ ,  $17\ \mu\text{m}$ , and  $19\ \mu\text{m}$  from the edge. Refer to Fig. 3 and Fig. 6(b) for definition of 'edge'.

## CLOCK OUTPUT

From the measured temperature induced frequency drift, we can extract using best fit to (1), the coefficients  $a$ ,  $b$  and  $c$  for the four resonators. Table 1 summarizes these numbers for the resonators presented in Fig. 8 (first measurement).

Table 1. Extracted coefficients  $a$ ,  $b$  and  $c$  for the best fit to first measurement of the four resonators shown in Fig. 8.

edge ( $\mu\text{m}$ )	Measured Turnover temperature ( $^{\circ}\text{C}$ )	Fitted coefficients		
		$a$	$b$	$c$
7	-30	-0.000391	-73.704291	19,737,789
13	0	-0.190434	96.863662	19,561,079
17	65	-0.296843	203.868377	19,425,545
19	85	-0.663465	475.433541	19,251,377

Taking the extracted coefficients in Table 1 for Resonators 2, 3 and 4 from Fig. 8, we can calculate  $k_1$  to be  $-0.4979$ ,  $k_3$  as  $-1.3202$  and  $k_{12}$  as  $-0.9041$ . Using the extracted  $k$  numbers, the output of the proposed system can be estimated using (5) and is plotted in Fig. 9. In order to evaluate the applicability of the one-time calibration, the same devices are measured against temperature a second time with the result

plotted in Fig. 8 using hollow symbols. The three lines in Fig. 9 represent the ideal clock output (solid line - no symbol) assuming the measured data exactly lies along a second-order polynomial, estimated clock output (dotted line - circle) using the first measurement data and the estimated clock output (dash dot - diamond) using the second set of measured data in Fig. 8. For both measurement sets, the temperature sensitivity of frequency is less than 10 ppm across  $-40^{\circ}\text{C}$  to  $85^{\circ}\text{C}$ .

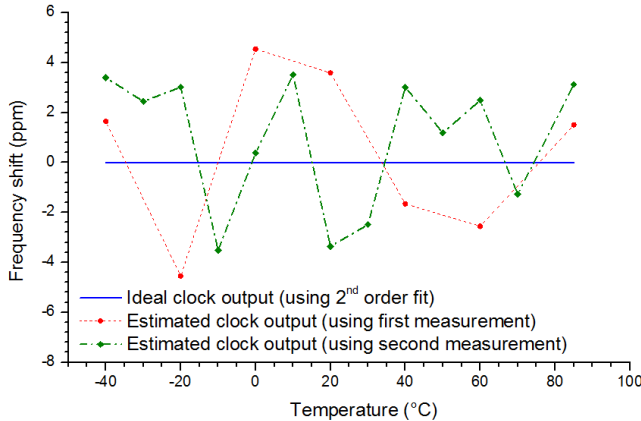


Figure 9: Relative frequency shift of the multi-resonator clock output (with Resonators 2, 3, and 4 in Fig. 8) in parts per million (ppm) as a function of temperature with first measurement (filled circles) and second measurement (filled diamonds). The estimated error of  $\sim 10$  ppm is due to the resonator frequency deviating from the ideal parabolic dependence on temperature. The solid line (no symbols) represents the ideal clock output assuming no deviation from pure second-order temperature dependence for the three resonators.

In order to evaluate the effect of calibration on the output of the multi-resonator clock if the calibration is not performed properly, the same analysis is repeated using Resonators 1, 2 and 3. As shown in Fig. 8, during the second temperature sweep, Resonator 1 was seen to have a relatively large shift in its frequency-temperature relation indicating measurement induced errors. Figure 10 plots the estimated clock output using resonators 1, 2, and 3 as the frequency inputs. The  $k$  values for this estimation were calculated from the first measurement in Fig. 8 for the same three devices ( $k_1=-0.4751$ ;  $k_2=1.3142$ ;  $k_3=3.8657$ ). As can be estimated from (10), the error in the two measurements for Resonator 1 leads to a second-order temperature dependence of the clock frequency output. Thus, achieving a temperature-stable clock output will necessitate use of stable resonators with repeatable frequency-temperature characteristics and a measurement setup capable of its accurate estimation.

## CONCLUSIONS

We report on a novel approach to enable temperature-stable frequency references for potential applications in navigation and time keeping. This system consists of multiple temperature-compensated resonators each having a unique temperature dependence of frequency. The system is analyzed for its sensitivity to measurement errors and the effects of such errors on the clock output have been quantified.

AlN-based piezoelectrically actuated and temperature-compensated ring resonators are used as a proof of concept for the proposed system. Using the proposed algorithm, we showed the compensated clock has a total temperature induced frequency shift of  $\sim 10$  ppm across a wide temperature range of  $-40^{\circ}\text{C}$  to  $+85^{\circ}\text{C}$ .

Compared to the performance of the individual resonators we note a  $\sim 20\times$  reduction in the total temperature induced frequency drift.

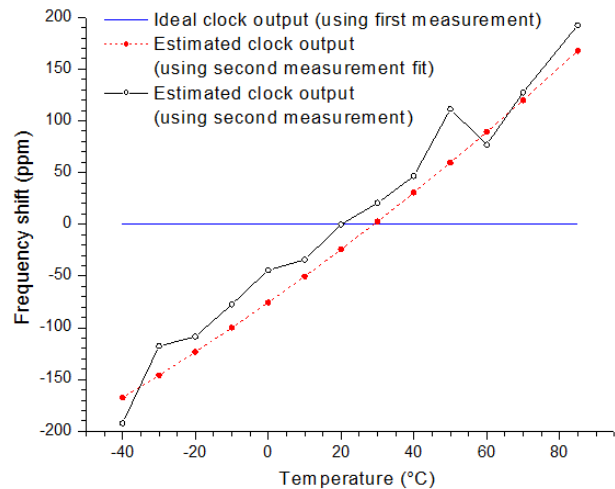


Figure 10: Relative frequency shift of the multi-resonator clock output (with Resonators 1, 2 and 3) in ppm as a function of temperature for three cases: (a) Ideal clock output using the fit to first measurement in Fig. 8. (b) Estimated clock output using the fit to second measurement. The error is due to the shift in the turnover characteristics of Resonator 1 between the first and second measurement. (c) Estimated clock output using the actual measured frequency vs. temperature characteristics from the second measurement in Fig. 8.

## ACKNOWLEDGEMENT

This work is supported by NASA under the Chip-Scale Precision Timing Unit project (Grant #NNX12AQ41G.) The authors acknowledge the support of the staff of the Lurie Nanofabrication Facility (LNF) at University of Michigan for their help with device fabrication.

## REFERENCES

- [1] R. Tabrizian, G. Casinovi and F. Ayazi, "Temperature-stable high-Q AlN-on-silicon resonators with embedded array of oxide pillars," *Hilton Head '10*, Hilton Head Island, SC, pp. 479-482, June 2010.
- [2] H. Lee, A. Partridge, and F. Assaderaghi, "Low jitter and temperature stable MEMS oscillators," *IEEE IFCS*, Baltimore, MD, pp.1-5, May 2012.
- [3] R. Melamud, *et al.*, "Temperature-compensated high-stability silicon resonators," *Appl. Phys. Lett.*, vol. 90, no. 24, pp. 244107, Jun. 2007.
- [4] V. Thakar, Z. Wu, A. Peczkalski, and M. Rais-Zadeh, "Piezoelectrically transduced temperature-compensated flexural-mode silicon resonators," *IEEE/ASME Journal of MEMS*, Vol. 22, No. 3, pp. 819-823, 2013.
- [5] V. Thakar, Z. Wu, C. Figueroa and M. Rais-Zadeh, "A temperature-stable clock using multiple temperature-compensated micro-resonators," *IEEE IFCS '14*, Taiwan, accepted (in press).
- [6] Z. Wu, *et al.*, "Piezoelectrically transduced high-Q silica micro resonators," *IEEE MEMS '13*, Taipei, Taiwan, pp.122-125, Jan. 2013.
- [7] V. A. Thakar and M. Rais-Zadeh, "Temperature-Compensated piezoelectrically actuated Lamé-mode resonators," *IEEE MEMS '14*, San Francisco, pp. 214-217, Jan. 2014.

## CONTACT

\*Vikram Thakar, tel: +1-734-355-3480; thakar@umich.edu